Experimental Thermal and Fluid Science 51 (2013) 10–17

Contents lists available at SciVerse ScienceDirect

Experimental Thermal and Fluid Science

journal homepage: www.elsevier.com/locate/etfs

Experimental study of heat transfer in a water film exposed to a radiant flux. Application to thermal protection of composite walls

Adrien Aubert [a], Fabien Candelier [a,b], Camille Solliec [a,*]

[a] DSEE, Ecole des Mines de Nantes, 4 rue Alfred Kastler, BP 20722, Nantes Cedex 3, France
[b] IUSTI, Université de la Méditerranée, 5 rue Enrico Fermi, 13453 Marseille Cedex 13, France

ARTICLE INFO

Article history:
Received 4 September 2012
Received in revised form 17 May 2013
Accepted 8 June 2013
Available online 3 July 2013

Keywords:
Water film
Protection
Heat transfer
Radiation
Composite wall

ABSTRACT

The following work is dedicated to assessing the performance of a falling water film as a thermal protection for composite walls exposed to a radiant flux. For this purpose, an experimental set-up was designed. The water film is created by spray nozzles and flow rates lie between 120 and 880 kg/hm$_{wall}$. Different radiant flux steps from 1 to 5 kW/m^2 are tested. Temperature is measured at different locations inside the composite panel and at the water inlet and outlet. Three different experiments are considered: one without water film, to serve as a reference, another where the composite and the film are exposed to the radiant flux without initial heating, and finally a wall at 100 °C before the film is triggered. The film shows a good capacity to cool and to protect the wall in the range of this study.

1. Introduction

New material research is a very active field. It represents for many industries the key to economic and energetic optimization. The maritime sector, for example, is radically impacted with developments of high performance composite materials. Their use provides weight, stability and energy consumption improvements to name but a few. However, despite suitable structural properties, some particular composites (based on fiber reinforced polymers) emit toxic fumes when submitted to important temperatures. Thus, they cannot be allowed for a number of internal applications for regulatory reason in case of fire [1].

Exception to this regulation can be made if a heat protection device is proved to prevent combustibility. This has motivated the present work. It is dedicated to the study of a water film based system. The idea is using important heat exchange with liquid film, when a vertical composite panel is submitted to a radiant heat flux.

Water films are indeed used in many thermal applications. They are found for example in seawater desalination device [2] or in the cooling systems of electronic components [3]. They are also used in the context of fire protection of oil tanks [4], glass [5] or metal walls [6]. Excellent heat removal properties were exhibited in these studies even for small water quantities. It is mostly done by convection. The high value of latent heat also allows a large amount of energy to be evacuated through vaporization. Finally, water semi transparency property leads to important radiation absorption capacity (in the infra-red mainly).

Despite the numerous studies concerning water film, its use in wall protection is still fairly limited to feasibility analysis and most often in unidimensional situations. This constitutes a lack of information for the development of protection device using water film.

This article proposes an experimental study of the thermal protection of a composite wall by a water film when submitted to a radiant heat flux. For this purpose an experimental test bench was developed. It allows the protection provided by the film along the wall to be studied for different flow rates and radiative heat fluxes. In order to cover a wide range of possible applications, three different experiments are tested when the wall is submitted to radiation.

2. Materials and methods

2.1. Wall description and instrumentation

In order to investigate the protection provided by the water film, temperature measurements are made inside the composite wall. Dimensions are 2.80 m height and 0.5 m width (noted respectively L and l). A cylindrical sample of the material is presented on Fig. 1. It is formed of a 40 mm thick core in balsa wood and of two skins of polyester resin and fiberglass (3 mm each) arranged on both sides. A total of 7 similar cylinders (20 mm diameter) was taken from a small sample of composite. In such pieces, a proper

* Corresponding author. Tel.:+332 51 85 82 65; fax: +332 51 85 82 99.
E-mail addresses: adrien.aubert@mines-nantes.fr (A. Aubert), fabien.candelier@univ-amu.fr (F. Candelier), camille.solliec@mines-nantes.fr (C. Solliec).

0894-1777/$ - see front matter © 2013 Elsevier Inc. All rights reserved.
http://dx.doi.org/10.1016/j.expthermflusci.2013.06.005

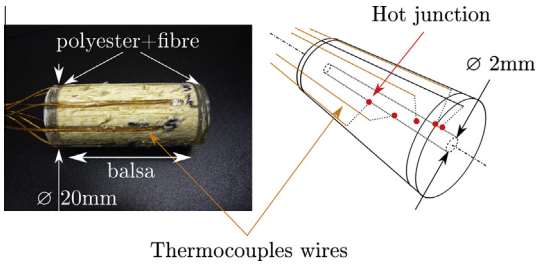

Fig. 1. Photo and schematic representation of a cylindrical sample of the composite wall equipped with thermocouples.

positioning of thermocouples at different depths is made easier. Holes are drilled in radial direction and staggered in a helical (45°) in the direction of cylinder length. The depth is limited to 9 mm, to avoid hot junctions alignment. K-type thermocouples are set in the composite at: 1, 2, 4, 8, 14, 24, 34 and 45.5 mm respectively to the side exposed to radiant flux. The temperature "probes" are then introduced into the composite test wall in a hole matching precisely the cylinder diameter. Sealing is ensured by a similar polyester resin.

Temperature "probes" were distributed on the test wall according to the scheme shown in Fig. 2. They are separated vertically with 42.5 cm (noted e) and spaced alternately horizontally around the center of the wall to reduce their number, while retaining the ability to observe three-dimensional phenomena (c = 2.5 cm).

2.2. Experimental apparatus

The test bench developed for this study is schematized in Fig. 2. Water is supplied by a centrifugal pump from a constant level tank. Flow rate is measured through a Coriolis flowmeter. The water film is created at the top of the wall by three flat spray nozzles (LECHLER, see Fig. 3). It is driven to the bottom of the plate by gravity. Water temperature is measured in the tank and also down the wall in the center of it (see the thermocouple position in Fig. 2).

The radiant heat flux is produced by 60 heating elements (250 W each) made of 904L stainless steel. The emissivity of such alloy is 0.9 at 200 °C and 0.97 at 500 °C [7] and can thus be considered to behave like a black body. A reflecting panel located behind aims to concentrate most of the radiation towards the test wall. Deflectors are used to avoid water projection on electrical connectors (see Fig. 4). The assembly is placed on a pivot. Note that in the later picture, heating elements are not oriented toward the test wall to facilitate the visualization. A sliding steel panel placed between the heating elements and the test wall is used to create steep steps of radiant heat flux. Finally, radiant heat flux density is measured on the wall by a CAPTEC fluxmeter and the corresponding surface temperature of the heating elements was measured by a thermocouple.

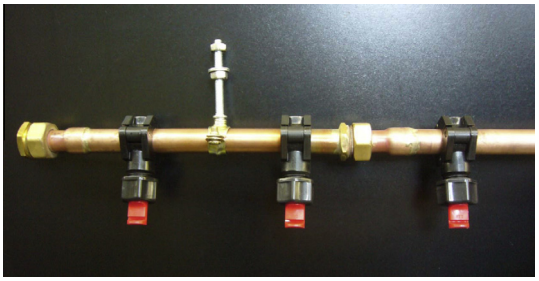

Fig. 3. Photograph of the water injection ramp equipped with three fat spray nozzles.

Fig. 5 presents the heat flux density received by the wall for different electric powers. Values are displayed as a function of height in the center of the wall only. The corresponding surface temperature of the heating elements are respectively 261, 340, 366 and 467 °C when the mean heat flux increases. Variations of radiant heat flux density at the top and the bottom of the wall can be noticed. They can be logically interpreted as a consequence of the view factor which decreases at these points. Nevertheless, for high radiant heat flux densities, fluctuations can be highlighted in the center of the wall. They can be explained by local differences in ohmic resistances of heating elements. They have been measured and standard deviation is non-negligible: 5.5 Ω.

This test bench enables us to study the effect of a water film flowing on a composite wall exposed to a radiant heat flux. Tendencies at high heat fluxes may be slightly influenced by the radiant heat flux non-homogeneity, but material conductivity tends to soften this effect.

2.3. Experimental procedure

Three different experimental categories were carried out. For each of them, the radiant heat source is used in steady state. This means heating resistances are powered at first and only once they

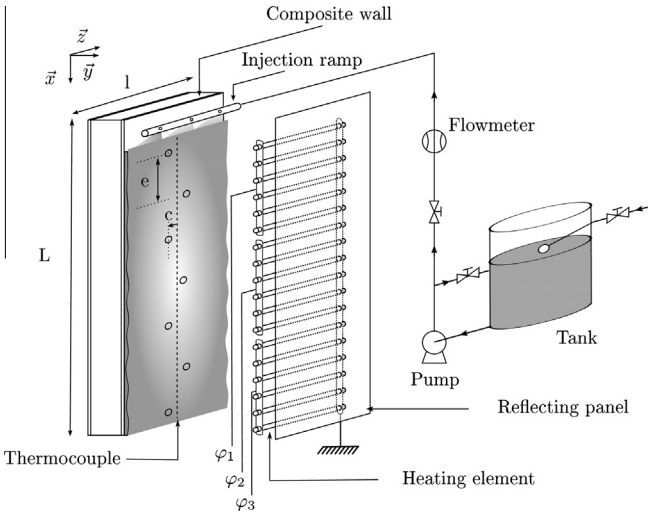

Fig. 2. Schematic view of the experimental test bench.

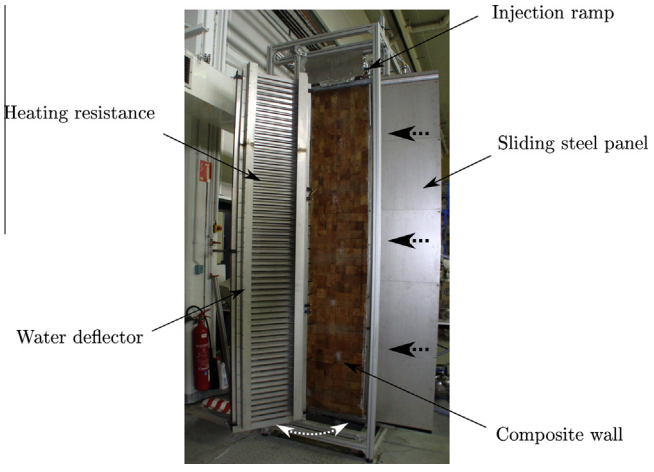

Fig. 4. Photograph of the experimental test bench.

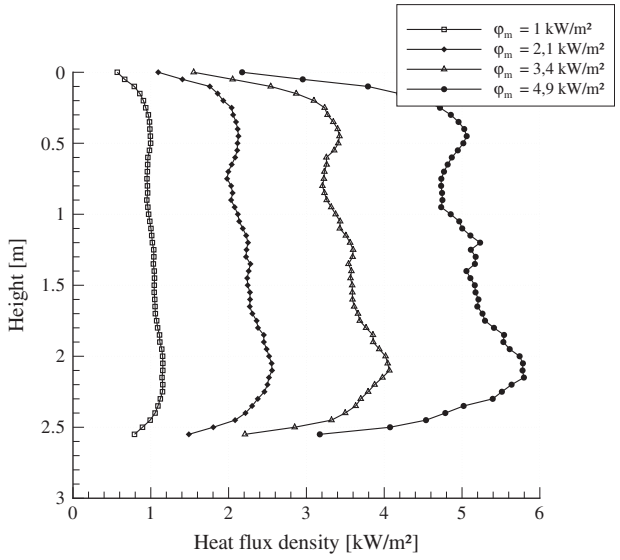

Fig. 5. Radiant heat flux densities measured in the center of the wall.

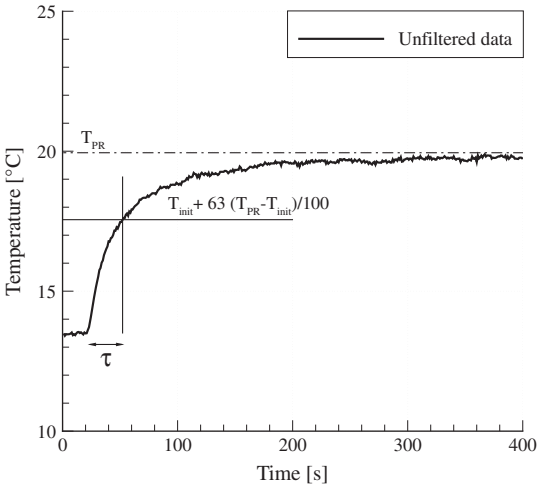

Fig. 6. Characteristic time determination.

are thermally established, measurements start. The wall is thus always submitted to a step of constant heat flux when the sliding panel is taken off.

- The first type of experiment aims at characterizing the wall response to an echelon of radiant heat flux. Temperature is measured in the wall. Once it reaches a steady state, experiment stops.
- The second type of experiment is performed with a pre-established water film on the wall. Thus the fluid just prevents the plate rise in temperature. Protection phenomenon is thereby uncoupled from the cooling aspect. Experiments start when the wall and the film are in steady state (they may have different initial temperatures). They are then submitted to a step of heat flux until an established state is reached, that is when experiment stops.
- Finally the third kind of experiment is intended to study the coupling between cooling and protection. The wall is thus submitted without water film to an echelon of flux. When it reaches a particular temperature (100 °C was arbitrarily chosen) the water film is triggered. Once more experiments last until the steady state is attained.

2.4. Results, treatments and normalization

Electric signals obtained by the thermocouples are submitted to different noise sources (electric, magnetic...). It was thus decided to filter them to estimate the temperature accurately. A second order Butterworth filtering is used. T_{PR} is then defined as the mean temperature once the steady state is reached. The characteristic time τ is defined as the time required by the system (wall or wall and film) to reach 63% of T_{PR} (see Fig. 6). This definition is arbitrary. It was taken by analogy with a first order system. It allows different configurations to be compared regarding the time needed to reach an established state. It is measured on the unfiltered data as filtering induces a time offset.

Power accumulated by the water film (P_{th}) is calculated using the water mass flow rate (Q_m), water heat capacity (C) and film temperature measurements in the tank (T_{tank}) and at the bottom of the plate (T_b).

$$P_{th} = Q_m C(T_b - T_{tank}). \quad (1)$$

As flow rate is taken constant, it is supposed that the mass loss due to evaporation is relatively small. This is coherent with the temperature reached by the film which is maximum 30 °C. Finally, a normalization of wall temperatures was necessary to give the best comparison between experiments. Thus temperature measured at the top of the wall is chosen to be zero in each experiment. Other measurements down the wall are given relatively to this temperature, so that they are noted ΔT. Comparisons are mainly done regarding temperature evolution along the plate. The absolute value of the temperature in the tank and at the top of the wall (T_{ref}) are provided in Table 1, to enable the real values of temperatures to be calculated.

2.5. Wall characterization

In order to characterize the behavior of the wall in a simplified configuration, an experiment was performed with a dry wall exposed to a step of radiant flux It brings some preliminary results that will later be compared to the results with the water film.

The temperature profile in steady state is presented as a function of height on Fig. 7. The values presented are measured by the thermocouples at 1 mm depth. Due to important sensitivity to heat, the composite wall has been tested for a single heat flux (1 kW/m^2). It would have been damaged for higher heat fluxes. Large temperature variations can be noticed with height (between 50 and 85 °C). Values are significantly correlated with the incident radiant heat flux. Although the temperature at the top of the wall is larger than at the bottom, while the radiative flux has the opposite behavior. This finding is possibly related to the stack effect. Natural convection thus may enhance the heating of the upper parts.

Another way to evaluate the behavior of the wall is the characteristic time defined in Section 2 and that is also presented in Fig. 7. Significant variations can be noted, extrema are 260 and 710 s. This could be linked to material properties evolution with temperature. Even though temperature variations are relatively small to explain such results. Therefore, it can be assumed that the characteristic time is modified by the presence of natural convection phenomena mentioned above (stack effect). The aforementioned natural convection seems to have a great effect on the results for the dry wall. It should not be relevant though in the presence of the water film. Indeed this phenomenon will be displaced at the free surface of the flow and will be reduced due to the surface renewal.

Table 1
Initial water temperature and reference temperature for each experiment on the composite wall.

	Heat flux densities (kW/m^2)															
	1				2,1				3,4				4,9			
Q (kg/h m_{wall})	600	300	150	120	600	450	390	300	600	450	390	330	690	630	570	450
T_{water} (°C)	21,7	16,4	18,5	19,2	21,8	15,8	14,1	17	22,0	12,9	13,7	15,7	12,7	12,7	13,4	13,9
T_{ref} (°C)	21,4	16,9	18,8	18,6	21,6	15,8	14,7	17	21,9	13,5	14,2	16,6	13,0	12,9	13,7	14,2

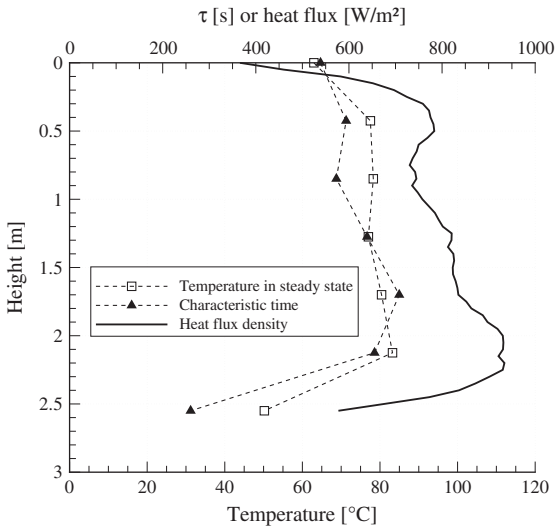

Fig. 7. Temperature profile in steady state and characteristic time for an unprotected wall submitted to a 1 kW/m^2 mean radiant heat flux as a function of the height.

2.6. Film drying

While performing experiments with the pre established water film, it has been noticed that in some particular configurations, after exposure to the radiant heat flux, the water film tended to dry in some small area (see Fig. 8). Evaporation is probably not the main cause of this mechanism as the temperature is low.

The phenomenon begins with a significant reduction in the thickness of the water film. It is initially localized in a very small area (about a centimeter square). Then, this zone extends downward and upward (symbolized by t^+ on the scheme). It finally reaches the top and the bottom of the wall. This observation suggests that the film becomes unstable under certain conditions of radiative fluxes and flows. This phenomenon was also observed in the case of a film heated by IR radiation flowing over a horizontal wall [8]. They have shown that this mechanism is triggered by Marangoni convection. A similar process may be involved here. Surface tension gradients appearing at the film surface (resulting from the radiant heat source) could lead to fluid migration and thus thinning of the film. Once this starts, the thinner zones of the film will tend to heat up more and sustain the mechanism. Finally the area increases in the vertical direction only as on the sides it is bounded by the film forced convection.

Experiments were conducted to estimate the appearance of this phenomenon for different flow rates and heat fluxes. The minimum flow rate value for the film to remain stable is depicted on Fig. 9. It is qualified as "critical". Radiant heat flux seems to affect the "critical" flow rate in a quasi-linear trend. Those values are taken as the lower limit for the flow rate in our experiments. This choice allows us to compare experiments that involve similar physical phenomena. However, each radiant heat flux has now a different flow range.

3. Results and discussion

3.1. Pre established film

As mentioned in the experimental procedure, the following results were obtained with an echelon of radiant flux on the wall and the water film initially in a thermally established state.

Fig. 10 shows the temperatures as a function of height (Flow rates are expressed in kilograms per hour per meter of wall width (kg/hm$_{wall}$), to account easily amounts of water necessary for the wall protection). They are measured at 1 mm depth. The temperature reference is presented in Table 1. Radiant heat flux density is 4.9 kW/m^2 and different flow rates are tested. Temperature profiles

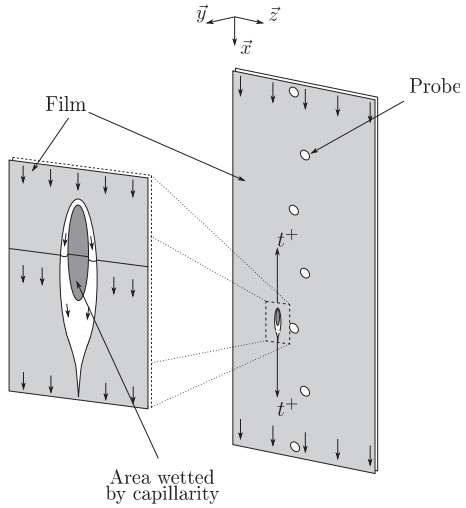

Fig. 8. Visual description of the unwetting phenomena.

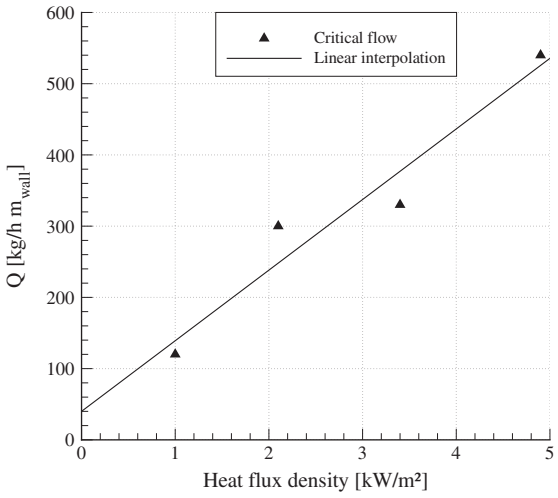

Fig. 9. Maximum unwetting flow rate versus radiant heat flux.

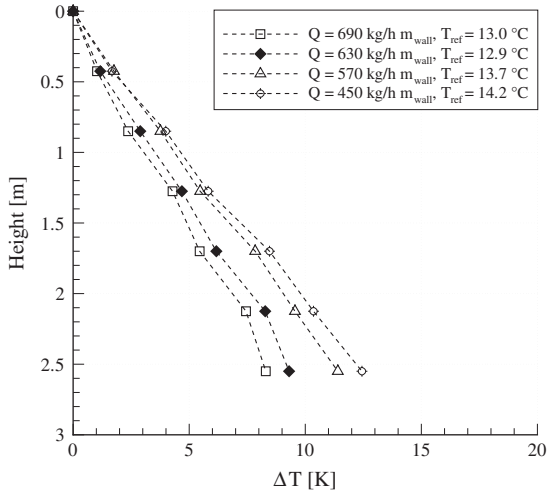

Fig. 10. Temperature profile in steady state with water film at different flow rates as a function of the height for 4.9 kW/m^2.

appear to be quasi-linear. Some small fluctuations around the general trend can be noticed. They can be explained by the staggered arrangement of temperature sensors in the wall. As expected, the higher the flow rate is, the lower the temperature. Similar results were observed with lower heat fluxes but are not presented here for reasons of brevity. Regarding the absolute values, wall temperature reaches a maximal value of 27 °C. At 1 kW/m^2, the maximum temperature reached is 32 °C for 120 kg/hm$_{wall}$. Note that 85 °C was obtained without water film in the same conditions. Water film thus appears to be very efficient to protect the wall. It gives a sharp decrease in temperature for a relatively small amount of water.

Another interesting value can be derived from these experiments. Fig. 11 shows the characteristic time depending on the height. The profiles are almost constant with height. Values obtained at the top of the wall are quite disparate though. This result is certainly related to the amplitude of temperature variation. Indeed this area undergoes only very small temperature variations that are of the same order of magnitude as the measurement noise. The results are presented for information purposes, but will be excluded from the analysis. In general, all the profiles converge around 25 s. For the wall without water film we obtained around 800 s, which is thirty time longer. Similar results were observed at lower heat fluxes. A possible understanding of this could be the following: whereas natural convection takes time to be fully developed in the dry wall case, convection is forced by the water film since the beginning of the experiments. Thus only the temperature of the film and the wall varies with time (natural convection at the film surface is assumed to be negligible as temperatures variation remains low). Besides, without water film, the physics changes along the experiments, thereby extending the transitory state.

Instead of studying separately the experiments for different radiant heat fluxes and flow rates, we decided to adopt the representation shown on Fig. 12. The temperature at the bottom of the wall (This is also the higher temperature, since the profile is linear and increasing) is presented versus the flow rate for every experiments realized. This helps to understand the influence of the flow rate on the temperature reached in steady state. The comparison between the different radiant heat fluxes is also made easier even though the range of flow rate is different due to drying of the film. In the case of low heat fluxes, temperature seems to be inversely proportional to the flow rate. It is thus possible to reduce the wall temperature by increasing slightly the flow rate in a first time, even though, the horizontal asymptotic behavior leads to less efficiency when the flow is important. Concerning the largest fluxes (3.4 and 4.9 kW/m^2), the comportment is not as monotone as previously. A change seems to occur passed a certain flow rate. See, for example the curve at 4.9 kW/m^2 for flow rates of 600 and 630 kg/hm$_{wall}$. After a certain flow value, temperature decreases more promptly. It could result from a change in the physics, leading to protection enhancement.

These results are to be analyzed together with the total power absorbed by the water film presented in Fig. 13. Indeed, if the wall temperature decreases, it can be either because the film absorbs or dissipates a greater amount of energy or due to a decrease of water temperature by increasing the flow rate. For weak heat fluxes, the power is only slightly dependent on the flow rate. The decrease in temperature of the wall can therefore be mainly attributed to using higher water quantity. Therefore temperature is reduced even if the power absorbed is still constant. For higher heat fluxes, influence of flow rate on the power is more important. A relatively constant power value is observed at first. It then rises and finishes decreasing for important flow rates.

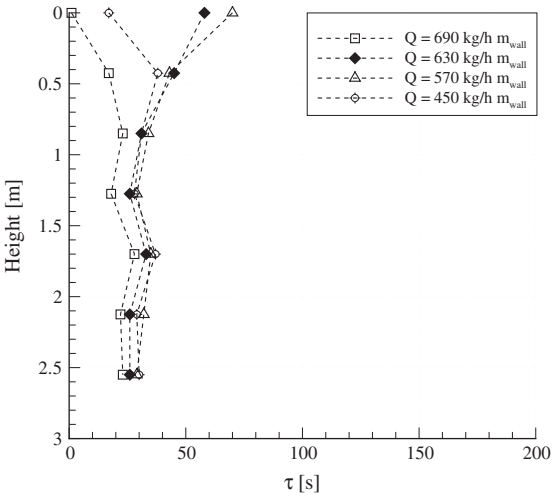

Fig. 11. Characteristic time profile for different radiative heat fluxes with water film as a function of the height for 4.9 kW/m^2.

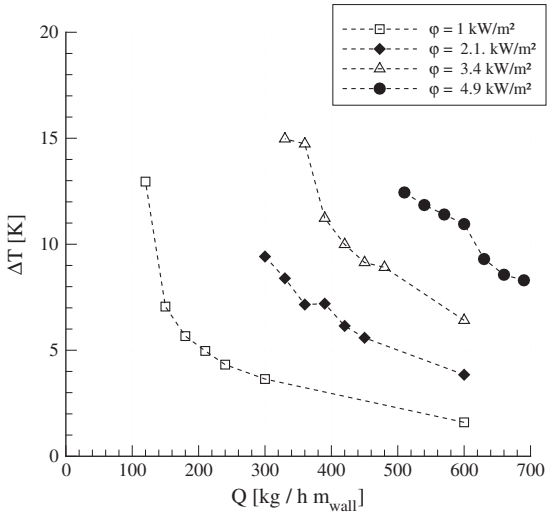

Fig. 12. Temperature at the bottom of the composite wall (255 cm) as a function of the flow rate for different heat fluxes.

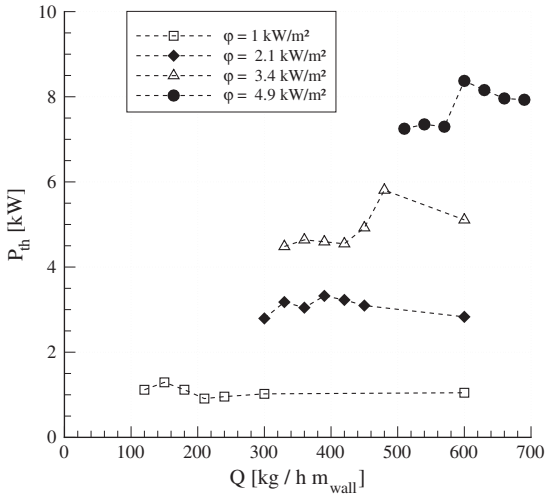

Fig. 13. Power accumulated by water on the composite wall as a function of the flow rate for different heat fluxes.

This can be explained by semi-transparency of water (absorption coefficient from [9] is presented on Fig. 14). Indeed, its absorptivity depends strongly on the wavelength of the radiation. It is almost transparent in the visible spectrum and tend to be opaque in the IR. After 3 μm the film can be considered as entirely absorbing the radiation at its free surface. Under 3 μm, according to Beer–Lambert law, the absorption of radiation is function of the film thickness.

Also in Fig. 14, the spectral distribution of the black body radiation at the surface temperature of the heating elements is presented. Assuming that the heating elements behave like a black body (see Section 2.2), it appears that, the spectral distribution of radiation tends to deviate to shorter wavelength as heat flux increases. For a given heat flux, increasing the film thickness can thus provide better absorption in the range 0–3 μm. The relative improvement potential can be estimated by integrating the emittance from 0 to 3 μm over the emittance integral over the whole spectrum. By doing so we obtained respectively 2%, 4.3%, 7.8% and 12% as the radiant heat flux increases. These fractions are coherent with the relative power increase observed on Fig. 13 as the flow rate increases. Increasing the flow rate that is also increasing the film thickness leads therefore to larger power absorption by the water film in the case of high radiant fluxes. Hence the wall temperature decreases faster. Finally for the highest flow rates, the film thickness is high enough to absorb much of the radiation and power is dissipated by interfacial transfers.

3.2. Film triggered on the wall at 100 °C

In the experiments presented previously, only the aspect of protection is considered. The water film prevents the wall from reaching too high temperatures, using mainly convection and water semi-transparent properties. However, as the wall is not exposed to the radiant source without water there is no effect of cooling of the wall induced by the film.

The following experiments aim to fill up this gap. The wall is first submitted to an echelon of radiant flux. The water film is triggered when the wall reaches 100 °C at $x = 2.55$ m. To ensure a quick wetting of the wall, experiments were made at higher flow rates than previously, 600, 752 and 880 kg/hm$_{wall}$ are used for each radiant heat fluxes excepted 1 kW/m^2 because it could not bring the wall at the triggering temperature (see Fig. 7). For better readability, temperatures are now presented in absolute value. Fig. 15 represents the evolution versus time of the temperature of the material at middle height (1.27 m) for different flow rates. Heat flux density is 2.1 kW/m^2. Three different thermocouples depths are considered: 1, 14 and 45.5 mm respectively to the face exposed to radiation. Curves have been off-setted in order to have a similar film triggering time. Differences in the first moments can be noticed. It corresponds to the phase when the wall is exposed to the heat flux without water film. The various experiments do not require the same exposure time to reach the criterion for triggering the film. The curve represented by dashes (- - -) reaches its maximum temperature after a less important heating time than the solid line (—). These differences could be explained by variations in initial temperature during the various experiments. This behavior can also be observed in Fig. 16, which isolates the temperature profiles in the material for the same probe at different times. The profiles at 400 s (the film is triggered at 720 s) show that the temperature differences may be of the order of 10°C. Also near the unexposed face (between 30 and 46 mm), temperature differences are reversed from those close to the exposed face. This observation tends to strengthen the fact that the higher the initial temperature is, the faster the wall reaches 100 °C. As a result,

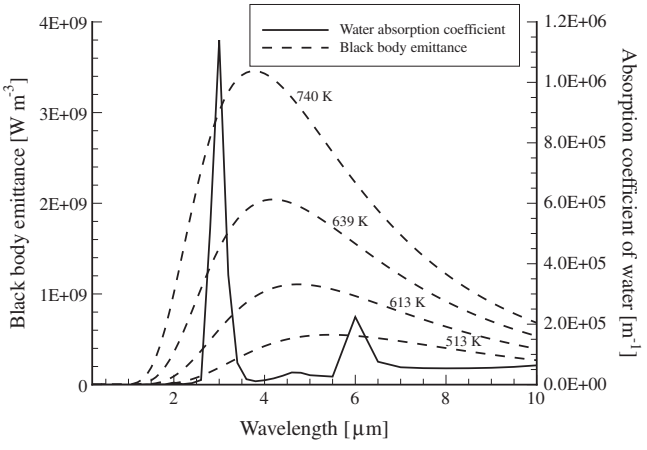

Fig. 14. Black body spectral radiant emittance for the surface temperature of the heating elements together with water absorption coefficient versus wavelength from [9].

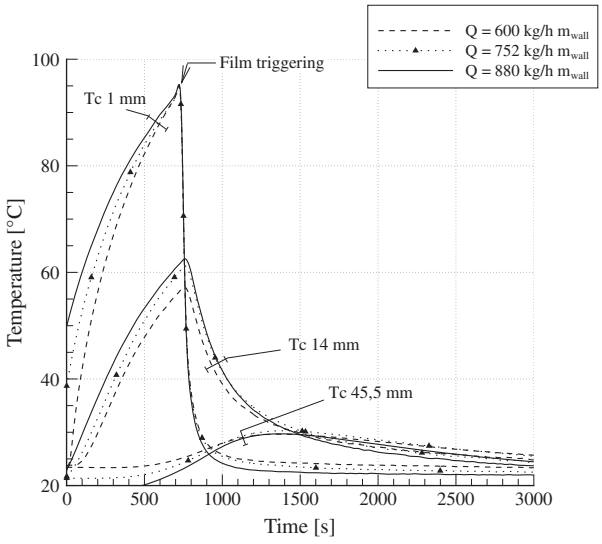

Fig. 15. Evolution as a function of time of the temperature of the wall at middle height for different flow rates and depths. Heat flux is 2.1 kW/m^2.

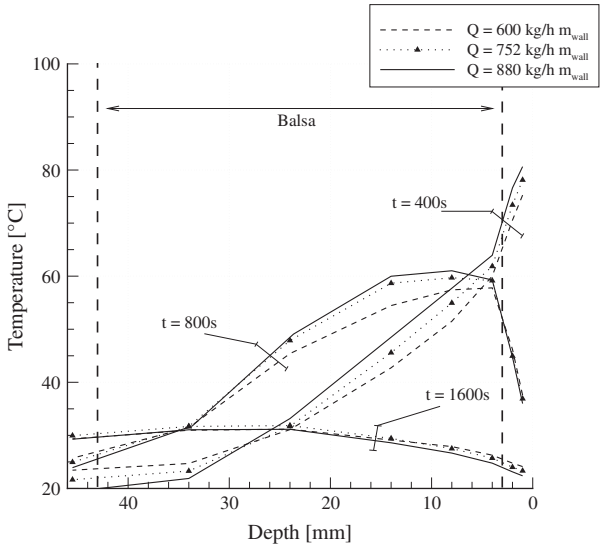

Fig. 16. Temperature profiles of the wall at middle height for different flow rates and times. Heat flux is 2.1 kW/m^2.

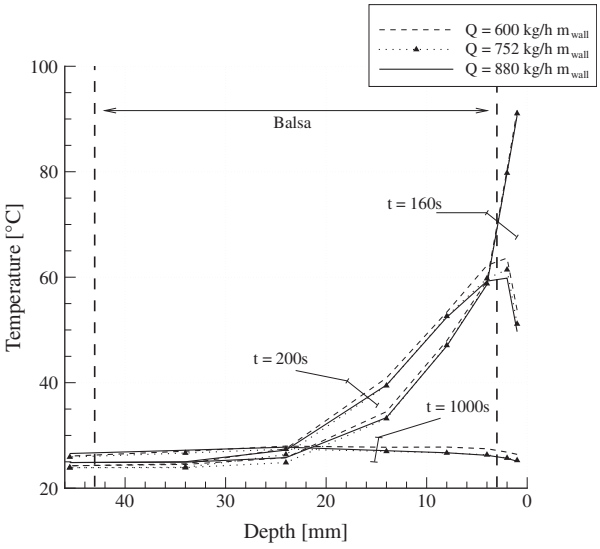

Fig. 18. Temperature profiles of the wall at middle height for different flow rates and times. Heat flux is 4.9 kW/m^2.

during the various tests, the wall has not accumulated the same amount of energy for similar heat flux density. For this reason analysis of these results is only focused on trends.

It can be noted in Fig. 15 that the cooling is very fast once the film is triggered. The wall temperature drops sharply to converge towards values inversely proportional to the flow rate. The impact of the film on the temperatures inside the material is off-setted by inertia effects. A phase shift can be observed according to the depth of the thermocouple considered. By comparing these results in terms of temperature profiles (see Fig. 16), it can be observed that 80 s after the start of the film (profiles at 800 s), the temperature of the face exposed to the radiation is lower than the temperature inside the material. In other words, the cooling of the wall by the water film is so fast that within seconds after the start of the film, heat transfer is partially reversed. After a quarter of an hour, the system is almost in a steady state.

Same remarks can be made for higher heat flux shown in Figs. 17 and 18. There are however some slight behavior differences. Indeed,

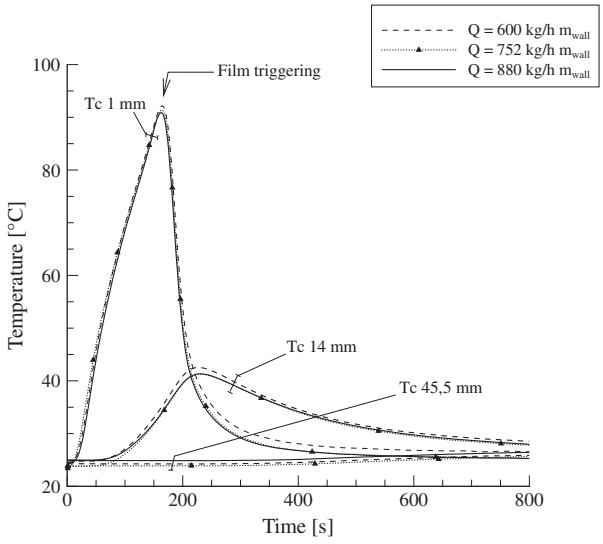

Fig. 17. Evolution as a function of time of the temperature of the wall at middle height for different flow rates and depths. Heat flux is 4.9 kW/m^2.

as the radiant heat flux is higher, the time required to achieve the criterion for triggering is smaller. Then fewer differences can be observed between the various tests regarding the heating phase and corresponding temperature profiles. On the other hand the material has accumulated less energy, the time required for the establishment of the system wall and film is much shorter.

4. Conclusions

In this article, heat transfer in a water film exposed to a radiant flux was studied experimentally. The emphasis was put on assessing the water film performance as a thermal protection for a composite wall. For this purpose, an original apparatus was set up. The radiant heat flux was produced by heating resistances. Flat spray nozzles allowed the film creation. Temperature measurements were performed by thermocouples inside the composite wall as well as in the water. Given the results, it appears that the wall can be maintained at low temperatures (around 30 °C) when exposed to heat fluxes until 5 kW/m^2. The temperature profile is thus quite linear with wall height. Obviously this can be achieved under certain water flow rate conditions. Experiments were performed in the range 120–700 kg/hm$_{wall}$. A major limit was found for low flow values due to partial unwetting of the wall, probably related to a thermo-capillary effect. This constitutes the main drawback of the system. Temperatures are globally still acceptable in the wetted parts but tend to increase dramatically in some small spots. Besides, the spectral distribution of radiation seems to be an important parameter to estimate the protection. As wavelengths near the visible is much less absorbed by water, flow rate must be in proportion increased for the highest radiant fluxes. Finally, experiments were performed with an initially heated wall. The water film produces a quick cooling of the wall.

Acknowledgments

This work has been performed within the MP08 project "Fire performance of composites for shipbuilding". The authors thank the financial support from the Pays de la Loire Region and the French State (Direction Générale des Entreprises, Délégation Générale de l'Armement), as well as all the other partners involved in this part of the Project (Bureau Veritas, DCNS, LNE, ISMANS, STX Europe).

References

[1] Solas, International Convention for the Safety of Life at Sea, Consolidated Edition, 2009.
[2] S. Ben Jabrallah, A. Belghith, J.P. Corriou, Convective heat and mass transfer with evaporation of a falling film in a cavity, International Journal of Thermal Sciences 45 (2006) 16–28.
[3] E.Y. Gatapova, O.A. Kabov, Shear-driven flows of locally heated liquid films, International Journal of Heat and Mass Transfer 51 (2008) 4797–4810.
[4] J.-M. Buchlin, Thermal shielding by water spray curtain, Journal of Loss Prevention in the Process Industries 18 (2005) 423–432.
[5] C.-W. Wu, T.-H. Lin, Full-scale evaluations on heat resistance of glass panes incorporated with water film or sprinkler in a room fire, Building and Environment 42 (2007) 3277–3284.
[6] Y. Lev, D.C. Strachan, A study of cooling water requirements for the protection of metal surfaces against thermal radiation, Fire Technology 25 (1989) 213–229.
[7] F. Cvena, Thermal Properties of Metals, ASM Materials Data Series, ASM, 2002.
[8] A. Ito, S.K. Choudhury, T. Fukano, Heated liquid film flow and its breakdown caused by Marangoni convection – the characteristic flow of pure water, JSME International Journal 33 (1990) 128–133.
[9] R. Siegel, J.R. Howell, Thermal Radiation Heat Transfer, Taylor & Francis, 2002.